PCCP

Accepted Manuscript

ROYAL SOCIETY OF CHEMISTRY

www.rsc.org/pccp

Forth-Back Oscillated Charge Carrier Motion in Dynamically Disordered Hexathienocoronene molecules: A Theoretical Study

K. Navamani and K. Senthilkumar*

Department of Physics, Bharathiar University, Coimbatore-641 046

*Corresponding author: ksenthil@buc.edu.in

Abstract

The electronic structure calculations were performed to investigate the charge transport properties of hexathienocoronene (HTC) based molecules. The effective displacement of the charge carrier along the π-orbital of nearby molecules is calculated by monitoring the forth and back oscillations of charge carrier through the kinetic Monte Carlo simulation. The charge transport parameters such as charge transfer rate, mobility, hopping conductivity, localized charge density, time average effective mass and degeneracy pressure are calculated and used to study the charge transport mechanism in studied molecules. The existence of degeneracy levels facilitates the charge transfer and is analyzed through degeneracy pressure. Theoretical results show that the site energy difference in the dynamically disordered system controls the forth-back oscillation of charge carrier and facilitates the unidirectional charge transport mechanism, along the sequential localized sites. The ethyl substituted HTC has good hole and electron hopping conductivity of 415 and 894 S/cm, respectively. The unsubstituted HTC has the small hole mobility of 0.06 cm^2/Vs which is due to large average effective mass, and is closer to the experimental results.

Key words

Site energy fluctuation, hopping conductivity, mobility, average effective mass, degeneracy pressure

1. Introduction

For the last three decades the organic electronics is an emerging field in science and technology[1-5] due to its potential applications in semiconducting devices such as field effect transistors,[6-8] photovoltaics,[9, 10] light emitting diodes[11, 12] and solar cells.[13-15] The organic materials and polymers are having soft degrees of freedom, structural flexibility and self-assembling property.[2, 3, 16-19] In addition to that, the potential advantages are less molecular weight, low cost processing, environmental compatibility and easily tunable electronic property through the chemical modifications makes the organic materials as more preferable for optoelectronic applications.[2, 5, 13, 20, 21] The weak intermolecular forces, low dielectric permittivity and structural disorder are responsible for large electron-phonon coupling and localized electronic states in the organic molecules.[22-25] In this case, the charge carrier is energetically relaxed by the surrounding nuclei of the thermally distorted molecule and is known as small polaron.[13, 16, 17, 25, 26] Therefore, the thermally activated hopping mechanism is used to describe the charge transfer (CT) process in the organic molecules[4, 24, 27-29] and the Marcus theory of charge transfer is used to study CT along the sequential sites.[20, 29-31] It has been shown in earlier studies that the nuclear dynamics is significant in the room temperature which results the breakdown of Franck-Condon (FC) principle.[1, 32-34] In the CT calculations, the nuclear dynamics is modeled as the harmonic oscillator and is coupled with the electronic degrees of freedom. The collection of harmonic oscillators dissipates the energy and hence the charge carrier is thermally activated.[22, 35] Hence, the charge transfer process in organic materials has the activation less barrier, that is, the nuclear dynamics relaxes the energy barrier between the neighboring molecules.[4, 26, 34] The earlier studies[4, 25, 26, 35, 36] show that the dynamic disorder decreases the electron-phonon coupling and increases the electronic interaction which facilitates the dynamic

localization and charge transfer. In this case, the charge transfer kinetics follows the intermediate regime between the adiabatic band transport and non-adiabatic hopping transport and is characterized by the effective disorder drift time,[16, 25] and the CT is termed as the "diffusion limited by dynamic disorder".

Generally, the device performance is strongly dependent on the charge carrier dynamics which is closely related with morphology and the electronic structure of the materials.[13, 20, 37, 38] Therefore, the current interest in organic electronics is synthesizing and characterizing an appropriate functional material on the basis of structure-property relationship and the substitution of hetero atoms and functional groups.[2, 3, 28, 37, 39, 40] In this work, the charge transport property of recently synthesized hexathienocoronene (HTC) molecules is studied.[41] These molecules have thiophene annealed coronene core with six double bonds in the periphery region which provides good thermal stability. The experimental study[41] shows that the HTC molecules have good self-aggregating property in the solid state and the phase transformation depends on the length of the alkyl side chains. As shown in Fig. 1, the HTC core has six thiophene rings and the presence of alkyl side chains in the HTC molecules decreases the steric repulsion which provides the better planarity. That is, the presence of alkyl side chains decreases the torsional disorder between thiophene and phenyl rings in the HTC molecule. The X-ray diffraction study reveals that HTC-b molecules are stacked with one another in columnar fashion and the intermolecular distance is 3.37 Å.[41] The grazing-incidence wide-angle X-ray scattering (GIWAXS) measurement reports that the HTC-b exists in crystalline phase and π-stacked arrangements are parallel to the surface. The experimental study[41] shows that the unsubstituted (HTC-a) and hexyl substituted HTC (HTC-b) are having high crystallinity. Field effect mobility in HTC-a and HTC-b in 0.002 and 0.001 cm^2/V s, respectively.[41] In the present work, we have studied the hole and electron

transport in these HTC molecules through the CT kinetic parameters such as rate of transition probability, hopping conductivity, mobility, average effective mass and degeneracy pressure which are obtained from electronic structure calculations, molecular dynamics and kinetic Monte Carlo simulations. The previous studies [17, 28, 38] show that the fluctuation of charge transfer integral and site energy with respect to nuclear degrees of freedom and orientation of nearby molecules introduces the forth-back oscillations of charge carrier in the tunneling regime. In the present study, the forth-back oscillations are studied on the basis of forward and backward rates and number of forward and backward oscillations.

2. Theoretical Formalism

By using tight binding Hamiltonian approach the presence of excess charge in a π-stacked molecular system is expressed as,[13, 42]

$$\hat{H} = \sum_i \varepsilon_i(\theta) a_i^+ a_i + \sum_{i \neq j} J_{i,j}(\theta) a_i^+ a_j \qquad (1)$$

where, a_i^+ and a_i are creation and annihilation operators, $\varepsilon_i(\theta)$ is the site energy, energy of the charge when it is localized at i^{th} molecular site and is calculated as diagonal element of the Kohn-Sham Hamiltonian, $\varepsilon_i = \langle \varphi_i | \hat{H}_{KS} | \varphi_i \rangle$, the second term of Equation (1), $J_{i,j}$ is the off-diagonal matrix element of Hamiltonian, $J_{i,j} = \langle \varphi_i | \hat{H}_{KS} | \varphi_j \rangle$ known as charge transfer integral or electronic coupling, which measures the strength of the overlap between φ_i and φ_j (HOMO or LUMO of nearby molecules *i* and *j*).

Based on the semi-classical Marcus theory, the CT rate (k) is defined as[29-31]

$$k = \frac{2\pi {J_{eff}}^2}{\hbar}\left(\frac{1}{4\pi\lambda k_B T}\right)^{1/2} \exp\left(-\frac{(\Delta\varepsilon_{ij}+\lambda)^2}{4\lambda k_B T}\right) \quad (2)$$

where, k_B is the Boltzmann constant, T is the temperature (here T=298 K), J_{eff} is the effective charge transfer integral, $\Delta\varepsilon_{ij}$ is the site energy difference between the nearby molecules, and λ is the reorganization energy. The generalized or effective charge transfer integral (J_{eff}) is defined in terms of charge transfer integral (J), spatial overlap integral (S) and site energy (ε) as,[43, 44]

$$J_{eff\,i,j} = J_{i,j} - S_{i,j}\left(\frac{\varepsilon_i + \varepsilon_j}{2}\right) \quad (3)$$

where, ε_i and ε_j are the energy of a charge when it is localized at i^{th} and j^{th} molecules, respectively. The site energy, charge transfer integral and spatial overlap integral are computed using the fragment molecular orbital (FMO) approach as implemented in the Amsterdam Density Functional (ADF) theory program.[18, 44, 45] In ADF calculation, we have used the Becke-Perdew (BP)[46, 47] exchange correlation functional with triple-ζ plus double polarization (TZ2P) basis set.[48] In this procedure, the charge transfer integral and site energy corresponding to hole and electron transport are calculated directly from the Kohn-Sham Hamiltonian.[13, 44]

The reorganization energy measures the change in energy of the molecule due to the presence of excess charge and changes in the surrounding medium. The reorganization energy due to the presence of excess hole (positive charge, λ_+) and electron (negative charge, λ_-) is calculated as,[13, 49, 50]

$$\lambda_{\pm} = \left[E^{\pm}\left(g^0\right) - E^{\pm}\left(g^{\pm}\right)\right] + \left[E^0\left(g^{\pm}\right) - E^0\left(g^0\right)\right] \quad (4)$$

where, $E^{\pm}\left(g^0\right)$ is the total energy of an ion in neutral geometry, $E^{\pm}\left(g^{\pm}\right)$ is the energy of an ion in ionic geometry, $E^0\left(g^{\pm}\right)$ is the energy of the neutral molecule in ionic geometry and $E^0\left(g^0\right)$

is the optimized ground state energy of the neutral molecule. The geometry of the studied molecules, HTC-a, HTC-b and HTC-c in neutral and ionic states are optimized using density functional theory method, B3LYP[51-53] in conjunction with the 6-31G(d,p) basis set, as implemented in the GAUSSIAN 09 package.[54]

The charge carrier mobility is calculated from diffusion coefficient, D by using the Einstein relation,[55]

$$\mu = \left(\frac{q}{k_B T} \right) D \tag{5}$$

The above classical Einstein relation is valid for disordered semiconducting materials when the system is under equilibrium condition. The previous studies show that the above relation is invalid when the system in non-equilibrium condition, such as FET under applied field, because the electric field dependent diffusivity is larger than the electric field response mobility.[56, 57]

In the present work, we assume that the charge carrier is initially localized on the molecule which is located at the center of the sequence of π-stacked molecules and the charge does not reach the end of molecular chain within the time scale of simulation due to the forth-back oscillations. In each step of Monte-Carlo simulation, the most probable hopping pathway is found out from the simulated trajectories based on the forward and backward charge transfer rates at particular conformation. In the case of normal Gaussian diffusion of the charge carrier in one dimension, the diffusion coefficient, D is calculated from effective displacement, d_{eff} and the total hopping time, τ_{Hop}

$$D = \frac{d_{eff}^2}{2\tau_{Hop}} = \frac{(|P_f - P_b| d)^2}{2\tau_{Hop}} \tag{6}$$

where, P_f and P_b are the probability for forward and backward motions of charge carrier and d is the distance between nearby π-stacked molecules. The hopping time for such oscillated motion along the CT path is defined as,[28] $\tau_{Hop} = \frac{N_f}{k_f} + \frac{N_b}{k_b}$. The forward and backward CT rates, k_f and $k_{b,}$ and number of forward and backward oscillations, N_f and N_b are numerically calculated by using kinetic Monte Carlo simulation. As reported in previous studies,[17, 28, 38] the site energy difference and dynamic disorder causes the forth-back oscillations of charge carrier in the tunneling regime. To calculate the forward and backward CT rates, the Marcus equation for CT rate given in Equation (2) is rewritten as,

$$k = \frac{2\pi {J_{eff}}^2}{\hbar}\left(\frac{1}{4\pi\lambda k_B T}\right)^{1/2} \exp\left(-\frac{\lambda}{4k_B T}\right)\exp\left(-\frac{\Delta\varepsilon_{ij}^2}{4\lambda k_B T}\right)\exp\left(-\frac{\Delta\varepsilon_{ij}}{2k_B T}\right) \qquad (7)$$

here, If $\Delta\varepsilon_{ij}$ is positive, $k \to k_b$; and if $\Delta\varepsilon_{ij}$ is negative, the k is k_f.

By comparing Equations (2) and (7), the ratio of forward and backward CT rates is equal to $\frac{k_f}{k_b} = \exp\left(-\frac{\Delta\varepsilon_{ij}}{k_B T}\right)$, as stated in the previous studies.[28, 38] Note that, the forth-back oscillations are purely depending on site energy difference and fluctuations in site energy. The earlier study[28] reports that the ratio of forward and backward CT rates is equal to the ratio of the number of forward and backward charge carrier oscillations, that is, $\frac{k_f}{k_b} = \frac{N_f}{N_b} = \exp\left(-\frac{\Delta\varepsilon_{ij}}{k_B T}\right)$. Therefore, the number of forward and backward oscillations are explicitly defined as, $N = \exp\left(-\frac{\Delta\varepsilon_{ij}^2}{4\lambda k_B T}\right)\exp\left(-\frac{\Delta\varepsilon_{ij}}{2k_B T}\right)$, here, $N = N_f$ when $\Delta\varepsilon_{ij}$ is negative and $N = N_b$ when $\Delta\varepsilon_{ij}$ is positive. As given in Equation (6), the effective displacement (d_{eff}) is calculated by using

probability for forward (P_f) and backward (P_b) oscillations and is written as $P_f = \left(\frac{k_f}{k_f + k_b} \right)$ and $P_b = \left(\frac{k_b}{k_f + k_b} \right)$.

The electronic and nuclear dynamics facilitates the density flux along the hopping sites and the time evolution of density flux gives the hopping conductivity (σ) as[58]

$$\sigma = \frac{3}{5} \varepsilon \frac{\partial P}{\partial t} \tag{8}$$

That is, the hopping conductivity is purely depending on the rate of transition probability and electric permittivity (ε) of the medium. The rate of transition probability for dynamically disordered system is calculated by using Master equation method and is written as[28, 38, 59]

$$\frac{\partial P_i}{\partial t} = \sum_i [P_{b,i} k_{b,i} - P_{f,i} k_{f,i}] \tag{9}$$

The intermolecular electrostatic interaction between the stacked molecules leads Frenkel excitonic splitting and facilitates the overlap of orbitals of nearby molecules.[14, 40, 60, 61] The dynamic disorder reduces the influences of electron-phonon scattering on localized charge carrier and hence the interaction between the electronic states is increased.[26] Here, the dynamic disorder leads to the Wannier delocalized excitonic splitting instead of pure Frenkel localized excitonic splitting [4, 22, 25, 35]. The degeneracy pressure is directly related with the orbital splitting and CT efficiency. The degeneracy pressure is calculated by using the average effective mass and localized charge density on the π-orbitals of nearby molecules and is written as[62]

$$P_d = \frac{\left(3\pi^2\right)^{2/3} \hbar^2}{5\left\langle m_{eff} \right\rangle} n^{5/3} \tag{10}$$

here, the distributed charge carrier density (n) on the π-orbitals is calculated as $n = \frac{\sigma}{e\mu}$, and its corresponding momentum and velocity are $k = \left(3\pi^2 n\right)^{1/3}$ and $v = \frac{d_{eff}}{\tau_{Hop}}$, respectively.[62] From the above relations, the average effective mass of the charge carrier is calculated as, $\left\langle m_{eff} \right\rangle = \frac{\hbar k}{v}$. Here, the average effective mass is the mass of the polaron in the distorted molecular geometry and is interacting continuously with the intermolecular forces and electronic and nuclear degrees of freedom.

To get the quantitative insight on charge transport properties of these molecules, the information about stacking angle and its fluctuation around the equilibrium is required. As reported in previous study,[33, 58] the equilibrium stacking angle and its fluctuation were calculated by using molecular dynamics (MD) simulation. The molecular dynamics simulation was performed for stacked dimers with fixed intermolecular distance of 3.37 Å for all HTC based molecules using NVT ensemble at temperature 298.15 K and pressure 10^{-5} Pa, using TINKER 4.2 molecular modeling package with the standard molecular mechanics force field, MM3. The simulations were performed up to 10 ns with time step of 1fs, and the atomic coordinates in trajectories were saved in the interval of 0.1 ps. The energy and occurrence of particular conformation were analyzed in all the saved 100000 frames to find the stacking angle and its fluctuation around the equilibrium value.

3. Results and Discussion

The geometry of the hexathienocoronene based molecules, HTC-a, HTC-b and HTC-c is optimized using DFT method at B3LYP/6-31G(d,p) level of theory and is shown in Fig. S1. The molecules HTC-b and HTC-c are differed by the substitution of alkyl side chains as C_6H_{13} and

C_2H_5 on the end thiophene rings, and for HTC-a molecule, the alkyl side chains were replaced by H atoms. In this work, the electronic structure calculations and MD simulations were performed for the studied HTC molecules with respective side chains and the results were used to study the charge carrier dynamics through the KMC method, as described in section 2. As the best approximation, the positive charge (hole) will migrate through the highest occupied molecular orbital (HOMO), and the negative charge (electron) will migrate through the lowest unoccupied molecular orbital (LUMO) of the stacked molecules, the charge transfer integral, spatial overlap integral and site energy corresponding to positive and negative charges are calculated based on orbital coefficients and energies of HOMO and LUMO. The density plot of HOMO and LUMO of the studied molecules calculated at B3LYP/6-31G(d,p) level of theory is shown in Figs. S2 and S3, respectively. As shown in Figs. S2 and S3, the HOMO and LUMO are π orbital and HOMO and LUMO are delocalized on the entire HTC core and very less density on the alkyl side chains of HTC-b and HTC-c molecules. The delocalization of HOMO and LUMO on the HTC core increases the π-stacking property through the π-π orbital interaction. The alkyl side chains substitution on HTC core does not significantly affect the delocalization of electron density on HOMO and LUMO, and effective charge transfer integral (see Figs. 2 and 3). That is, in the π-stacked molecules, the overlap of nearby HTC cores will facilitate both hole and electron transport along the columnar axis, and these molecules may have ambipolar character.

3.1. Effective Charge Transfer Integral

The effective charge transfer integral (J_{eff}) for hole and electron transport in the studied HTC based molecules is calculated by using Equation (3). The previous studies[18, 33] show that the J_{eff} strongly depends on π-stacking distance and π-stacking angle. The experimental result[41] shows that the intermolecular distance between two molecules in the stacked dimer is 3.37 Å for

HTC-b molecule. Therefore, the J_{eff} for hole and electron transport in the HTC based molecules is calculated with fixed stacking distance of 3.37 Å and the stacking angle is varied from 0 to 90º in the step of 10º. The variation of J_{eff} with respect to stacking angle for hole and electron transport in the studied HTC molecules is shown in Figs. 2 and 3, respectively. The shape and distribution of frontier molecular orbital on each monomer are responsible for the orbital overlap between the neighboring π-stacked molecules. As observed in Figs. S2 and S3, HOMO and LUMO are delocalized on the entire HTC core which leads the significant effective charge transfer integral for both hole and electron transport. As observed in Fig. 2, for hole transport, the maximum J_{eff} of around 0.48 eV is calculated at the stacking angle range of 45-50º. At these stacking angles, the distance between the sulfur atoms of nearby molecules is around 2.9 Å which facilitate the stronger interaction between the π-stacked molecules. At these π-stacking angles, the HOMO of each monomer contributes nearly equally for HOMO of the dimer. For example, at 50º of stacking angle, the HOMO of the HTC-a dimer consists of HOMO of first monomer by 49% and the second monomer by 50% which leads the constructive overlap between the π-orbitals. The significant J_{eff} of 0.32 eV is observed at the stacking angles of 40 and 60º for hole transport (see Fig. 2 and Table S1). This is because of the constructive overlap between HOMO of each monomer while forming the HOMO of dimer. It has been found that the introduction of alkyl side chains does not affect the J_{eff} significantly. The substitution of alkyl chains on the HTC core enhances the planarity of the molecule. It has been found that the J_{eff} for hole transport is minimum at the stacking angles of 20 and 70º. This is because of the unequal contribution of HOMO of each monomer on the HOMO of the stacked dimer. For instance, the J_{eff} calculated for hole transport at 70º of stacking angle is below 0.01 eV, at this angle the

HOMO of HTC dimer consists 87 % HOMO of first monomer and 12% HOMO of second monomer.

It has been observed that the maximum effective charge transfer integral (J_{eff}) for electron transport in the HTC molecule is 0.41 eV at 70º of stacking angle. At this angle, the LUMO of the dimer consists of LUMO of first monomer by 48% and the second monomer by 51% which leads the constructive overlap. As shown in Fig. 3 and Table S1, at 20 and 90º of stacking angle the J_{eff} value for electron transport is nearly equal to zero which is due to the destructive overlap of LUMO of each monomer in the dimer system. Notably, at the stacking angle of 40º, the studied molecules are having significant J_{eff} value in the range of 0.15 - 0.25 eV for both hole and electron transport. The MD results show that the equilibrium stacking angle for unsubstituted HTC (HTC-a), hexyl substituted HTC (HTC-b) and ethyl substituted HTC (HTC-c) is 60º, 45º and 55º, respectively, and the stacking angle fluctuation up to 10 to 15º from the equilibrium stacking angle is observed (see Fig. S4). That is, the substitution of alkyl side chains on the HTC core reduces the equilibrium stacking angle. The change in J_{eff} due to the stacking angle fluctuation is included while calculating the CT kinetic parameters through kinetic Monte-Carlo simulation.

3.2. Site Energy Difference

Site energy difference is one of the key parameters that determines the rate of CT and is equal to the difference in site energy ($\Delta\varepsilon_{ij} = \varepsilon_j - \varepsilon_i$) of nearby π-stacked molecules. The site energy difference arises due to the conformational disorder, electrostatic interactions and polarization effects. The previous studies[28, 38, 58] show that the site energy difference ($\Delta\varepsilon_{ij}$) provides the significant impact on charge carrier dynamics and is acting as the driving

force for forward motion when $\Delta\varepsilon_{ij}$ is negative, and is acting as a barrier for forward motion when $\Delta\varepsilon_{ij}$ is positive, that is, the carrier takes the backward drift due to the positive value of $\Delta\varepsilon_{ij}$. The change in site energy difference with respect to the stacking angle for hole and electron transport in the studied molecules is shown in Figs. 4 and 5. It has been found that the stacking angle fluctuation has significant effect on the $\Delta\varepsilon_{ij}$, except for electron transport in C_6H_{13} substituted HTC upto 40º of stacking angle. At 0º of stacking angle, $\Delta\varepsilon_{ij}$ is zero for both hole and electron transport. For both hole and electron transport in unsubstituted HTC and C_2H_5 substituted HTC molecules, the maximum value of $\Delta\varepsilon_{ij}$ is nearly 0.05 eV at 80º of stacking angle and minimum value is nearly -0.05 eV at the stacking angle of 40º. For hole transport, at equilibrium stacking angle the molecules HTC, HTC-b and HTC-c have the site energy difference of around 0.01, 0.02 and -0.02 eV, respectively, and for electron transport the site energy difference is 0.02, 0.06 and 0.05 eV (see Figs. 4 and 5). The calculated $\Delta\varepsilon_{ij}$ values at different stacking angles were included while calculating the CT rate and other kinetic parameters through Monte-Carlo simulation. In the present study, the change in $\Delta\varepsilon_{ij}$ due to the stacking angle variation is responsible for forth-back oscillations along the π-stacked molecules and is analyzed through forward and backward CT rate, as described in Section 2.

3.3. Reorganization Energy

The change in energy of the molecule due to structural reorganization by the presence of excess charge will act as a barrier for charge transport. The geometry of neutral, anionic and cationic states of the studied HTC based molecules were optimized at B3LYP/6-31G(d,p) level of theory and the reorganization energy is calculated by using Equation (4).

It has been observed that the unsubstituted HTC (HTC-a) molecule has maximum reorganization energy value of 0.23 eV for the presence of excess positive charge. By analyzing the optimized geometry of neutral and cationic states of HTC molecule, we found that the presence of positive charge alters the torsional angle between the thiophene and phenyl rings of HTC core up to 3º which is the reason for the high hole reorganization energy. The substitution of alkyl side chains on the HTC molecule decreases the reorganization energy up to 0.1 eV for hole transport and hence HTC-b and HTC-c molecules have minimum hole reorganization energy of around 0.13 eV. It has been found that the HTC, HTC-b and HTC-c molecules have similar reorganization energy of around 0.14 eV for the presence of excess negative charge. Notably, the HTC core consists of circularly fused phenyl rings attached with six thiophene rings which make the planarity, core rigidity and responsible for small structural relaxation due to the presence of excess negative charge and hence the electron reorganization energy is minimum for the studied HTC molecules.

3.4. Charge Carrier Dynamics

The calculated charge transport key parameters such as effective charge transfer integral, site energy difference, reorganization energy and structural fluctuation in the form of stacking angle distribution are used to study the charge carrier dynamics through the kinetic Monte Carlo simulations. In the present model, forth-back oscillations of a charge carrier effect on charge carrier motion in the tunneling regime are studied. The structural fluctuation and its effect on site energy difference are responsible for the forward and backward CT. As observed in previous studies,[32, 33, 58] the survival probability of a charge carrier corresponding to forward and backward transports has been calculated from kinetic Monte Carlo simulation, and is shown in Figs. 6 and 7. As mentioned in previous Section, the forward and backward CT rates, number of

forward and backward oscillations, probability for forward and backward oscillations, effective displacement, total hopping time, rate of transition probability, average effective mass and degeneracy pressure are calculated and are used to study the charge carrier dynamics in the studied HTC molecules. As shown in Fig. 6, the forward and backward hole transfer rates in HTC-a are comparable, whereas in HTC-c the forward CT rate is higher by three orders of magnitude than the backward rate.

As given in Table 1, the effective rate of hole transfer and hopping conductivity in the HTC-a, HTC-b and HTC-c molecules are 1.3 $x10^{14}$, 1.17$x10^{15}$ and 7.82$x10^{15}$/s and 6.9, 62.1 and 415 S/cm, respectively. The presence of side chains in HTC molecule decreases the hole reorganization energy by 0.1 eV which enhances the CT rate and hopping conductivity (see Table 1). The J_{eff} for hole transport in the studied HTC-c molecule is nearly 0.45 eV at equilibrium stacking angle of 55º (see Fig. 2) which is also responsible for good hole transporting ability. The fluctuation in stacking angle is around 40-70º, for HTC-c molecule, and the variation in effective electron transfer integral is in the range of 0.15 - 0.42 eV and calculated electron reorganization energy is 0.14 eV which enhances the effective electron transfer rate and hopping conductivity as 1.68$x10^{16}$/s and 894 S/cm, respectively (see Table 2). It has been found that the calculated average effective mass of polaron for both hole and electron transport is much heavier than the free electron mass (see Tables 1 and 2), which is in agreement with the previous study.[25] That is, the effective mass of the polaron is infinite when it is localized in the distorted molecules, due to less electronic coupling and larger electron-phonon coupling.[25] Böhlin et al.[26] noticed that in the presence of dynamical disorder, the localized charge carrier is less influenced by the electron-phonon coupling (reorganization energy) as compared in the ideal system. The effect of static and dynamic fluctuation on charge transport in Donor-Bridge-Acceptor systems is

studied by Yuri A Berlin et al.[32] and they concluded that the dynamic fluctuation facilitates the band-like transport due to the self-averaging effect of electronic coupling or effective charge transfer integral. Therefore, the dynamic disorder controls the effective mass of the polaron which enhances the charge transfer. For instance, the average effective mass of the polaron for electron transport in the HTC-c molecules is less than the other studied HTC molecules (see Table 2), due to less electron-phonon coupling (~0.14 eV) and larger values of fluctuated electronic coupling (0.15-0.42 eV). The number of forward and backward oscillations, probability for forward and backward oscillations of a charge carrier and average site energy difference while including the structural fluctuations in kinetic Monte Carlo simulation are summarized in Table S2. It has been observed that number of forward oscillations is higher than the backward oscillations for hole and electron transport in ethyl substituted HTC (HTC-c) molecule and their probability for forward charge carrier motion is 0.76 and 0.91, respectively. That is, the probability for forward motion of a charge carrier is comparably higher than that of backward motion which increases the forward transport along the π-stacked molecules, and hence the ethyl substituted HTC molecule (HTC-c) has good ambipolar charge transport character (see Tables 1 and 2). Here, the significant effective charge transfer integral and small reorganization energy reduces the charge localization time on the frontier molecular orbital (HOMO or LUMO) and the calculated average effective mass of hole and electron at HTC-c is comparably small (2.67×10^{-30} and 2.26×10^{-30} kg). In this case, the calculated average site energy difference corresponding to forward and backward oscillations for hole transport is -0.054, 0.052 eV and for electron transport it is -0.13, 0.13 eV, respectively. As given in Table S2, the number of forward oscillations corresponding to hole and electron transport in HTC-c is relatively higher

than the number of backward oscillations, and the effective displacement (d_{eff}) of a charge carrier in the forward direction is higher in HTC-c molecule.

The hexyl substituted HTC (HTC-b) has the stacking angle fluctuation in the range of 30-60º around the equilibrium angle of 45º and the variation in J_{eff} is in the range of 0.1-0.45 eV which leads the significant charge transporting ability. It has been found that HTC-b has significant hole and electron mobility of 1 and 1.63 cm^2/V s and calculated average effective mass of hole and electron in HTC-b is $1.51x10^{-29}$ and $1.21x10^{-29}$ kg, respectively. The number of forward and backward oscillations corresponding to hole transport in HTC-b is 1.14 and 0.84 and for electron transport it is 1.37 and 0.87, respectively. The calculated total time for hopping process in the HTC-b and HTC-c for hole transport is 0.51, 0.42 fs and for electron transport it is 0.65 and 0.53 fs, respectively. The number of forward and backward oscillations corresponding to hole and electron transport in unsubstituted HTC (HTC-a) are nearly equal and hence the charge carrier oscillates longer time before hopping to the next molecule (see Table 1 and 2). In this case, the calculated average site energy difference corresponding to forward and backward oscillations for hole transport is -0.005, 0.005 eV and for electron transport it is -0.007, 0.007 eV, respectively. As observed in Table S2, the probability for forward and backward oscillations of a charge carrier in HTC-a is nearly equal which increases the average effective mass and decreases the effective displacement (d_{eff}) and charge transporting ability. The calculated hole mobility is 0.06 cm^2/V s which is higher than the experimental field effect mobility of 0.002 cm^2/V s. The previous studies show that the experimentally measured mobility depends on substrate and substrate temperature[63-65] and FET mobility is field dependent and non-equilibrium diffusion. However, theoretically calculated mobility by the Einstein relation is field independent and is based on equilibrium thermal diffusion process. Here the carrier is strongly

localized on the molecular site and the calculated localized charge density is $6.53x10^{26}/m^3$. The above results clearly show that the site energy difference in the geometrically fluctuated molecules controls the forth-back oscillation of charge carrier and facilitate the unidirectional charge transfer process (see Tables 1, 2 and S2). It has been found that the site energy difference in the dynamically disordered systems is acting as the driving force for unidirectional the charge transport mechanism. That is, the forward and backward charge carrier hopping network is controlled or tuned by the site energy difference, which is in agreement with the previous studies.[28, 38]

To get further insight on charge transport in the studied molecules, the degeneracy pressure is calculated by using Equation (10). The existence of degeneracy levels promotes the delocalization of charge carrier and is calculated as degeneracy pressure. The previous studies[26, 32] show that the localized charge carrier on the dynamically disordered system is less influenced by the electron-phonon scattering and the CT mechanism follows the static non-Condon effect. The weak electron-phonon scattering in the dynamically disordered system increases the coupling strength between the electronic states which leads the intermediate CT mechanism between the localized hopping transport and delocalized band transport. The calculated degeneracy pressure is summarized in the Tables 1 and 2. It has been found that the high degeneracy pressure drifts the carrier from one localized site to another localized site. Among the studied molecules, HTC-c has comparably maximum degeneracy pressure of $4.34x10^5$ and $6.24x10^5$ Pa for hole and electron transport which favors the charge transport. Here, the orbital splitting follows the Wannier type and carrier is delocalized on the frontier molecular orbitals. In the case of HTC-a molecule, the degeneracy pressure for hole dynamics is relatively small ($7.35x10^4$ Pa) and the charge transporting ability of HTC-a is weak. In this case, the splitting of

energy levels follows the Frenkel type and charge carrier takes the large number of forth-back oscillations. The degeneracy pressure for hole and electron transport in the HTC-b molecule is significant and the values are 2.9×10^5 and 2.37×10^5 Pa, respectively, which facilitate the CT process.

4. Conclusion

The charge transport properties of hexathienocoronene (HTC) based molecules are investigated by using electronic structure calculations. The structural fluctuation effect on effective charge transfer integral and site energy difference is included while studying the charge carrier dynamics through the kinetic Monte Carlo simulations. The number of forward and backward oscillations and probability for forward and backward oscillations are calculated from the kinetic Monte Carlo simulation and are used to study the dynamics of the charge carrier along the π-stacked molecules. The charge transfer parameters such as effective charge transfer rate, hopping conductivity, mobility, localized charge density, average effective mass and degeneracy pressure were calculated and the dynamic disorder effect on charge transport in the HTC molecules is studied. It has been found that the site energy difference in the dynamically disordered system is acting as the driving force for unidirectional charge carrier propagation. The ethyl and hexyl substituted HTC (HTC-c and HTC-b) molecules have good ambipolar transporting ability. The unsubstituted HTC molecule (HTC-a) has the small hole mobility of 0.06 cm^2/V s which is due to the strong localization of positive charge on the molecular site and large effective mass and is in agreement with the previous experimental results.

Acknowledgement: The authors thank the Department of Science and Technology (DST), India for awarding research project under Fast Track Scheme.

Supporting Information

Optimized structures of unsubstituted hexathienocoronene (HTC-a), hexyl substituted hexathienocoronene (HTC-b), ethyl substituted hexathienocoronene (HTC-c) molecules are given in Fig. S1. Highest Occupied Molecular Orbitals (HOMO) and the Lowest Unoccupied Molecular Orbitals (LUMO) of the studied HTC-a, HTC-b and HTC-c molecules are given in Figs. S2 and S3 respectively. The plot between the number of occurrence, potential energy with respect to stacking angle calculation from molecular dynamics simulation for unsubstituted HTC (HTC-a) molecule is given in Fig.S4. The effective charge transfer integral (J_{eff}) at different stacking angle (θ) for hole and electron transport in the studied HTC-a, HTC-b and HTC-c molecules are summarized in Table S1. The number of forward (N_f) and backward (N_b) oscillations and their probabilities (P_f and P_b), effective displacement (d_{eff}) and average site energy difference $\left\langle \Delta\varepsilon_{ij} \right\rangle$ corresponding to forward and backward charge carrier motions calculated from kinetic Monte Carlo simulation for hole and electron transport are summarized in Table S2.

References

1 W. Zhang, W. Liang and Y. Zhao, *J. Chem. Phys.*, 2010, **133**, 024501.
2 D. Andrienko, J. Kirkpatrick, V. Marcon, J. Nelson and K. Kremer, *Phys. stat. sol.(b)*, 2008, **245**, 830-834.
3 V. Marcon, J. Kirkpatrick, W. Pisula and D. Andrienko, *Phys. stat. sol.(b)*, 2008, **245**, 820-824.
4 D. L. Cheung and A. Troisi, *Phys. Chem. Chem. Phys.*, 2008, **10**, 5941-5952.
5 S. E. Koh, B. Delley, J. E. Medvedeva, A. Facchetti, A. J. Freeman, T. J. Marks and M. A. Ratner, *J. Phys. Chem. B*, 2006, **110**, 24361-24370.
6 H. E. Katz, *J. Mater. Chem.*, 1997, **7**, 369-376.
7 H. E. Katz, A. J. Lovinger, J. Johnson, C. Kloc, T. Siegrist, W. Li, Y. Y. Lin and A. Dodabalapur, *Nature*, 2000, **404**, 478-481.
8 M. Shim, A. Javey, N. W. Shi Kam and H. Dai, *J. Am. Chem. Soc.*, 2001, **123**, 11512-11513.
9 N. S. Sariciftci, L. Smilowitz, A. J. Heeger and F. Wudl, *Science*, 1992, **258**, 1474-1476.
10 X. Zhan, Z. Tan, B. Domercq, Z. An., X. Zhang, S. Barlow, Y. Li, D. Zhu, B. Kippelen and S. R. Marder, *J. Am. Chem. Soc.*, 2007, **129**, 7246-7247.
11 J. H. Burroughes, D. D. C. Bradley, A. R. Brown, R. N. Marks, K. Mackay, R. H. Friend, P. L. Burns and A. B. Holmes, *Nature*, 1990, **347**, 539-541.
12 C. W. Tang and S. A. Vanslyke, *Appl. Phys. Lett.*, 1987, **51**, 913-915.
13 F. C. Grozema and L. D. A. Siebbles, *Int. Rev. Phys. Chem.*, 2008, **27**, 87 -138.
14 S. Mohakud and S. K. Pati, *J. Mater. Chem.*, 2009, **19**, 4356-4361.
15 X. Yang, L. Wang, C. Wang, W. Long and Z. Shuai, *Chem. Mater.*, 2008, **20**, 3205-3211.
16 L. Wang and D. Beljonne, *J. Phys. Chem. Lett.,*, 2013, **4**, 1888-1894.
17 L. Wang, Q. Li, Z. Shuai, L. Chen and Q. Shi, *Phys. Chem. Chem. Phys.*, 2010, **12**, 3309-3314.
18 P. Prins, K. Senthilkumar, F. C. Grozema, P. Jonkheijm, A. P. H. J. Schenning, E. W. Meijer and L. D. A. Siebbles, *J. Phys. Chem. B*, 2005, **109**, 18267-18274.
19 X. Feng, V. Marcon, W. Pisula, R. Hansen, J. Kirkpatrick, F. Grozema, D. Andrienko, K. Kremer and K. Mullen, *Nat. Mater.*, 2009, **8**, 421.
20 J. L. Bredas, D. Beljonne, V. Coropceanu and J. Cornil, *Chem. Rev.*, 2004, **104**, 4971.
21 Y.-A. Duan, Y. Geng, H.-B. Li, X.-D. Tang, J.-L. Jin and Su. Zhong-Min, *Organic Electronics*, 2012, **13**, 1213-1222.
22 R. D. Pensack and J. B. Asbury, *J. Phys. Chem. Lett.*, 2010, **1**, 2255-2263.
23 W. Q. Deng and W. A. Goddard, *J. Phys. Chem. B*, 2004, **108**, 8614-8621.
24 J. L. Bredas, J. P. Calbert, D. A. d. S. Filho and J. Cornil, *Proc. Natl. Acad. Sci.*, 2002, **99**, 5804-5809.
25 A. Troisi, *Chem. Soc. Rev*, 2011, **40**, 2347-2358.
26 J. Bohlin, M. Linares and S. Stafstrom, *Phys. Rev. B*, 2011, **83**, 085209.
27 B. Baumeier, J. Kirkpatrick and D. Andrienko, *Phys. Chem. Chem. Phys.*, 2010, **12**, 11103-11113.
28 J. Kirkpatrick, V. Marcon, K. Kremer, J. Nelson and D. Andrienko, *J. Chem. Phys.*, 2008, **129**, 094506.
29 A. A. Kocherzhenko, F. C. Grozema, S. A. Vyrko, N. A. Poklonski and L. D. A. Siebbeles, *J. Phys. Chem. C*, 2010, **114**, 20424-20430.

30 A. Troisi, A. Nitzan and M. A. Ratner, *J. Chem. Phys.*, 2003, **119**, 5782-5788.
31 D. P. McMahon and A. Troisi, *Phys. Chem. Chem. Phys.*, 2011, **13**, 10241-10248.
32 Y. A. Berlin, F. C. Grozema, L. D. A. Siebbeles and M. A. Ratner, *J. Phys. Chem. C*, 2008, **112**, 10988-11000.
33 K. Navamani, G. Saranya, P. Kolandaivel and K. Senthilkumar, *Phys. Chem. Chem. Phys.*, 2013, **15**, 17947-17961.
34 S. S. Skourtis, I. A. Balabin, T. Kawatsu and D. N. Beratan, *Proc. Natl. Acad. Sci. USA*, 2005, **102**, 3552-3557.
35 A. Troisi and D. L. Cheung, *J. Chem. Phys.*, 2009, **131**, 014703.
36 A. Troisi and G. Orlandi, *Phys. Rev. Lett.*, 2006, **96**, 086601.
37 M. Jaiswal and R. Menon, *Polym Int*, 2006, **55**, 1371-1384.
38 V. Ruhle, A. Lukyanov, F. May, M. Schrader, T. Vehoff, J. Kirkpatrick, B. Baumeier and D. Andrienko, *J. Chem. Theory Comput.*, 2011, **7**, 3335-3345.
39 L. Lin, H. Geng, Z. Shuai and Y. Luo, *Organic Electronics*, 2012, **13**, 2763-2772.
40 S. Mohakud, A. P. Alex and S. K. Pati, *J. Phys. Chem. C*, 2010, **114**, 20436-20442.
41 L. Chen, S. R. Puniredd, Y. Z. Tan, M. Baumgarten, U. Zschieschang, V. Engelmann, W. Pisula, X. Feng, H. Klauk and K. Mullen, *J. Am. Chem. Soc.*, 2012, **134**, 17869-17872.
42 E. A. Silinsh, *Organic Molecular Crystals, Springer - Verlag, Berlin*, 1980.
43 M. D. Newton, *Chem. Rev.*, 1991, **91**, 767-792.
44 K. Senthilkumar, F. C. Grozema, F. M. Bichelhaupt and L. D. A. Siebbeles, *J. Chem. Phys.*, 2003, **119**, 9809-9817.
45 G. Te Velde, F. M. Bickelhaupt, E. J. Baerends, C. Fonseca Guerra, S. J. A. Van Gisbergeh, J. G. Snijders and T. Ziegler, *J. Comput. Chem.*, 2001, **22**, 931-967.
46 A. D. Becke, *Phys. Rev. A*, 1988, **38**, 3098-3100.
47 J. P. Perdew, *Phys. Rev. B*, 1986, **33**, 8822-8824.
48 J. G. Snijders, P. Vernooijs and E. J. Baerends, *At. Data Nucl. Data Tables*, 1981, **26**.
49 H. L. Tavernier and M. D. Fayer, *J. Phys. Chem. B*, 2000, **104**, 11541-11550.
50 M. M. Torrent, M. Durkut, P. Hadley, X. Ribas and C. Rovira, *J. Am. Chem. Soc.*, 2004, **126**, 984-985.
51 S. H. Vosko, L. Wilk and M. Nusair, *Can. J. Phys.*, 1980, **58**, 1200-1211.
52 A. D. Becke, *J. Chem. Phys.*, 1993, **98**, 5648-5652.
53 C. T. Lee, W. T. Yang and R. G. Parr, *Phys. Rev. B*, 1988, **37**, 785-789.
54 M. J. Frisch, G. W. Trucks, H. B. Schlegel, G. E. Scuseria, M. A. Robb, J. R. Cheeseman, G. Scalmani, V. Barone, B. Mennucci, G. A. Petersson, H. Nakatsuji, M. Caricato, X. Li, H. P. Hratchian, A. F. Izmaylov, J. Bloino, G. Zheng, J. L. Sonnenberg, M. Hada, M. Ehara, K. Toyota, R. Fukuda, J. Hasegawa, M. Ishida, T. Nakajima, Y. Honda, O. Kitao, H. Nakai, T. Vreven, J. A. Montgomery, Jr., J. E. Peralta, F. Ogliaro, M. Bearpark, J. J. Heyd, E. Brothers, K. N. Kudin, V. N. Staroverov, R. Kobayashi, J. Normand, K. Raghavachari, A. Rendell, J. C. Burant, S. S. Iyengar, J. Tomasi, M. Cossi, N. Rega, J. M. Millam, M. Klene, J. E. Knox, J. B. Cross, V. Bakken, C. Adamo, J. Jaramillo, R. Gomperts, R. E. Stratmann, O. Yazyev, A. J. Austin, R. Cammi, C. Pomelli, J. W. Ochterski, R. L. Martin, K. Morokuma, V. G. Zakrzewski, G. A. Voth, P. Salvador, J. J. Dannenberg, S. Dapprich, A. D. Daniels, O. Farkas, J. B. Foresman, J. V. Ortiz, J. Cioslowski and D. J. Fox, *Gaussian 09, Revision B.01, Gaussian, Inc. Wallingford CT.*, 2009.
55 L. B. Schein and A. R. McGhie, *Phys. Rev. B: Condens. Matter Mater. Phys.*, 1979, **20**, 1631-1639.

56 Y. Roichman and N. Tessler, *Appl. Phys. Lett.*, 2002, **80**, 1948-1950.
57 G. A. H. Wetzelaer, L. J. A. Koster and P. W. M. Blom, *Phys. Rev. Lett.*, 2011, **107**, 066605.
58 K. Navamani and K. Senthilkumar, *J. Phys. Chem. C*, 2014, **118**, 27754-27762.
59 Z. G. Yu, D. L. Smith, A. Saxena, R. L. Martin and A. R. Bishop, *Phys. Rev. Lett.*, 2000, **84**, 721-724.
60 A. Datta, S. Mohakud and S. K. Pati, *J. Mater. Chem.*, 2007, **17**, 1933-1938.
61 A. Datta, S. Mohakud and S. K. Pati, *J. Chem.. Phys.*, 2007, **126**, 144710.
62 D. J. Griffiths, *Introduction to Quantum mechanics, Pearson Education*, 2005, 230-260.
63 S. Ando, R. Murakami, J. Nishida, H. Tada, Y. Inoue, S. Tokito, S. Tokito and Y. Yamashita, *J. Am. Chem. Soc.*, 2005, **127**, 14996.
64 S. Ando, J. Nishida, Y. Inoue, S. Tokito and Y. Yamashita, *J. Mater. Chem.*, 2004, **14**, 1787.
65 S. Ando, J. Nishida, H. Tada, Y. Inoue, S. Tokito and Y. Yamashita, *J. Am. Chem. Soc.*, 2005, **127**, 5336.

Table 1 Rate of transition probability $\left(\frac{\partial P}{\partial t}\right)$, hopping conductivity (σ), total hopping time (τ_{Hop}), mobility (μ), π-electron density (n), time average effective mass $\left(\left\langle m_{eff}(t)\right\rangle\right)$ and degeneracy pressure (P_d) for hole transport in hexathienocoronene molecules, HTC-a, HTC-b and HTC-c.

Molecules	$\frac{\partial P}{\partial t}$ (fs^{-1})	σ (S/cm)	τ_{Hop} (fs)	μ (cm^2/Vs)	n ($\times10^{26}$ m^{-3})	$\left\langle m_{eff}(t)\right\rangle$ ($\times10^{-30}$ kg)	P_d ($\times10^{5}$ Pa)
HTC-a (R=H)	0.13	6.9	2.16	0.06	6.53	142.4	0.73
HTC-b (R=C_6H_{13})	1.17	62.1	0.51	1	3.88	15.1	2.92
HTC-c (R=C_2H_5)	7.82	415	0.42	14.86	1.74	2.67	4.34

Table 2 Rate of transition probability $\left(\frac{\partial P}{\partial t}\right)$, hopping conductivity (σ), total hopping time (τ_{Hop}), mobility (μ), π-electron density (n), time average effective mass $\left(\left\langle m_{eff}(t)\right\rangle\right)$ and degeneracy pressure (P_d) for electron transport in hexathienocoronene molecules, HTC-a, HTC-b and HTC-c.

Molecules	$\frac{\partial P}{\partial t}$ (fs^{-1})	σ (S/cm)	τ_{Hop} (fs)	μ (cm^2/Vs)	n ($\times10^{26}$ m^{-3})	$\left\langle m_{eff}(t)\right\rangle$ ($\times10^{-30}$ kg)	P_d ($\times10^{5}$ Pa)
HTC-a (R=H)	0.49	26	1.04	0.54	3.1	26.46	1.08
HTC-b (R=C_6H_{13})	1.51	80.2	0.65	1.63	2.8	12.1	2.37
HTC-c (R=C_2H_5)	16.8	894	0.53	28.54	1.96	2.26	6.24

Figure Captions:

Fig. 1: The chemical structure of hexathienocoronene (HTC) based molecules (HTC-a: R′ = H, HTC-b: R′ = C_6H_{13} and HTC-c**:** R′ = C_2H_5).

Fig. 2: The effective charge transfer integral (J_{eff}, in eV) for hole transport in HTC-a (solid line), HTC-b (dotted line) and HTC-c (dashed line) molecules at different stacking angles (θ, in degree)

Fig. 3: The effective charge transfer integral (J_{eff}, in eV) for electron transport in HTC-a (solid line), HTC-b (dotted line) and HTC-c (dashed line) molecules at different stacking angles (θ, in degree)

Fig. 4: The site energy difference ($\Delta\varepsilon_{ij}$, in eV) for hole transport in HTC-a (solid line), HTC-b (dotted line) and HTC-c (dashed line) molecules at different stacking angles (θ, in degree)

Fig. 5: The site energy difference ($\Delta\varepsilon_{ij}$, in eV) for electron transport in HTC-a (solid line), HTC-b (dotted line) and HTC-c (dashed line) molecules at different stacking angles (θ, in degree)

Fig. 6: The survival probability of a positive charge at particular site corresponding to forward and backward transports with respect to time in (a) HTC-a (b) HTC-b and (c) HTC-c molecules

Fig. 7: The survival probability of a negative charge at particular site corresponding to forward and backward transports with respect to time in (a) HTC-a (b) HTC-b and (c) HTC-c molecules

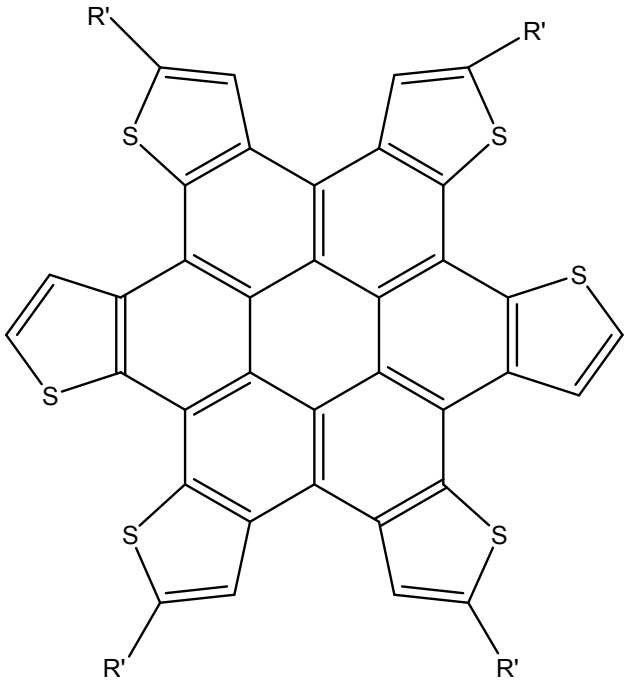

Fig. 1

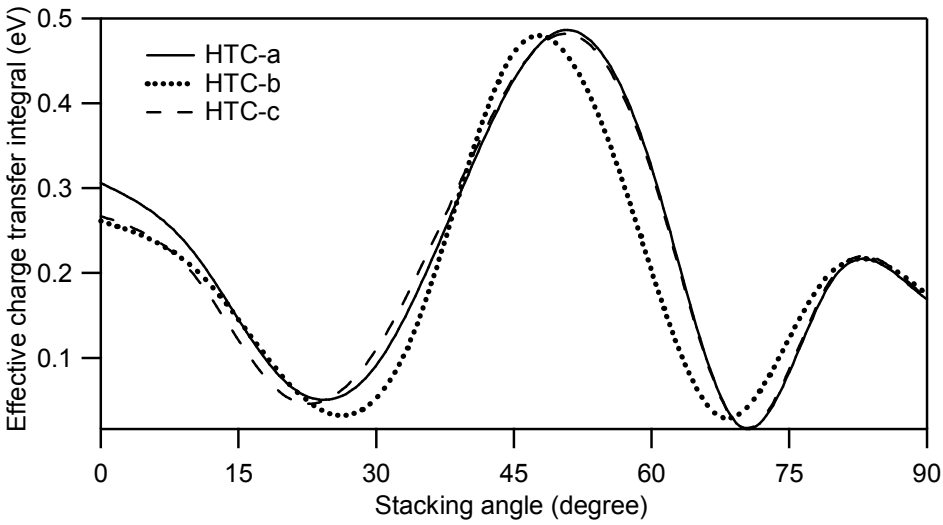

Fig. 2

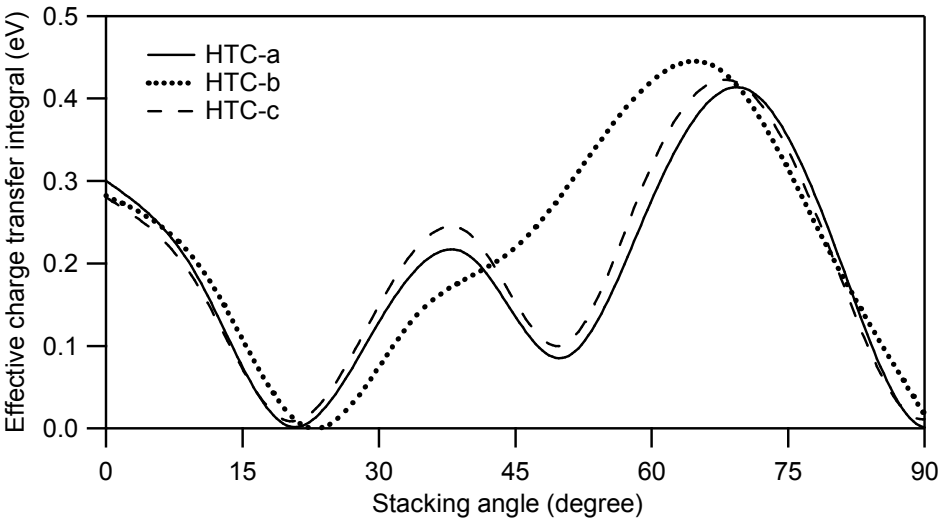

(b)

Fig. 3

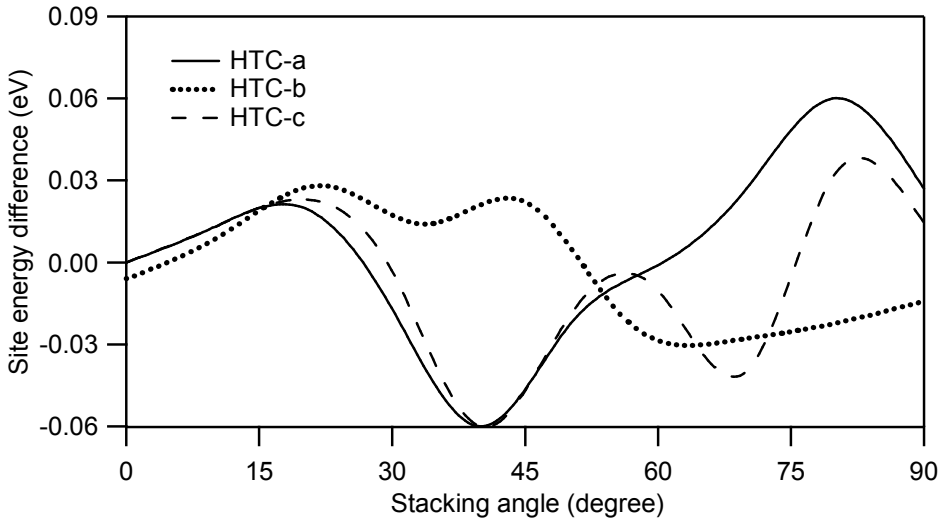

Fig. 4

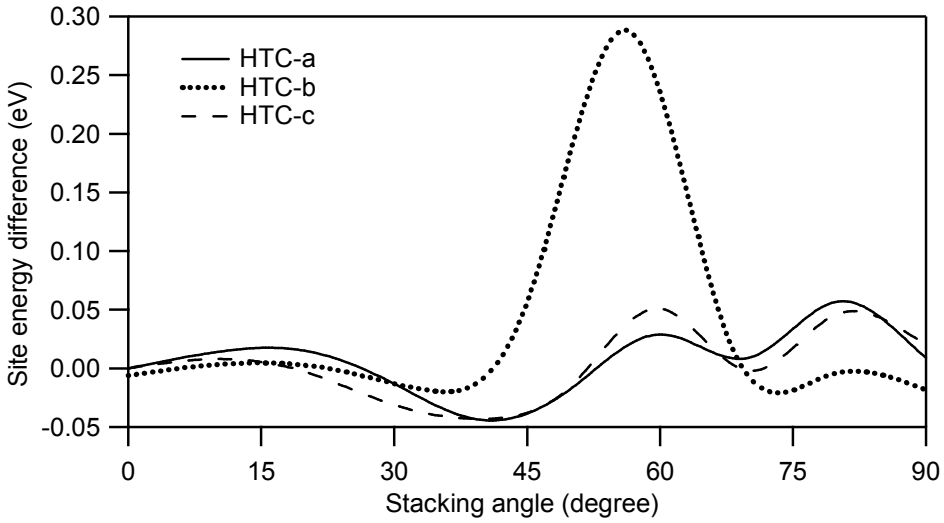

Fig. 5

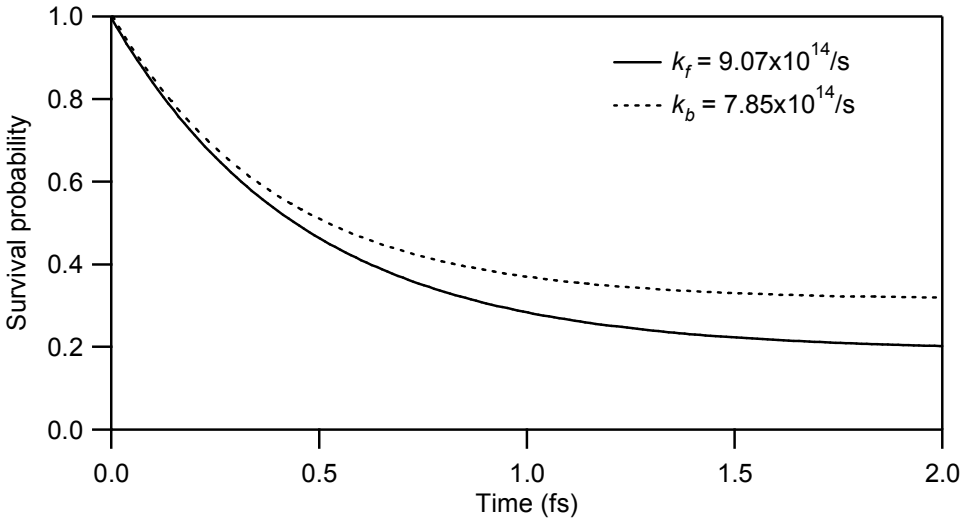

(a)

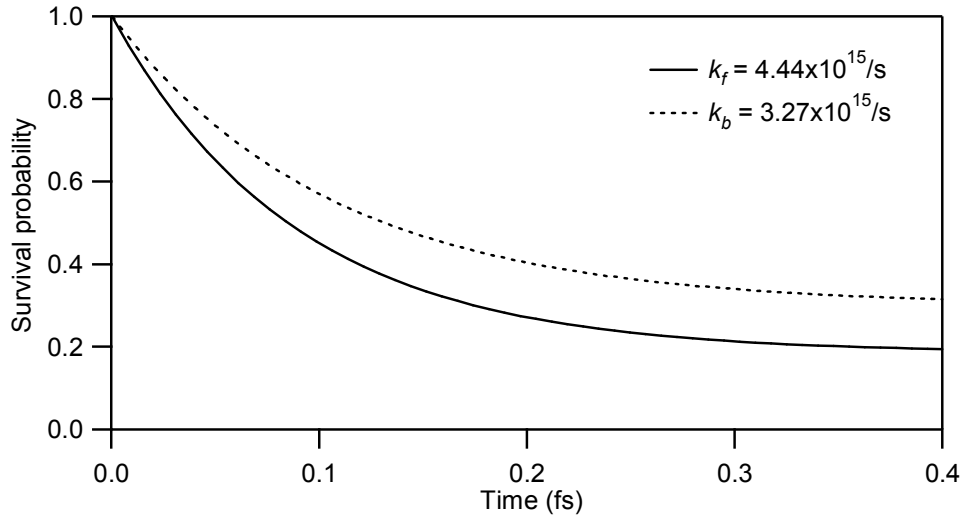

(b)

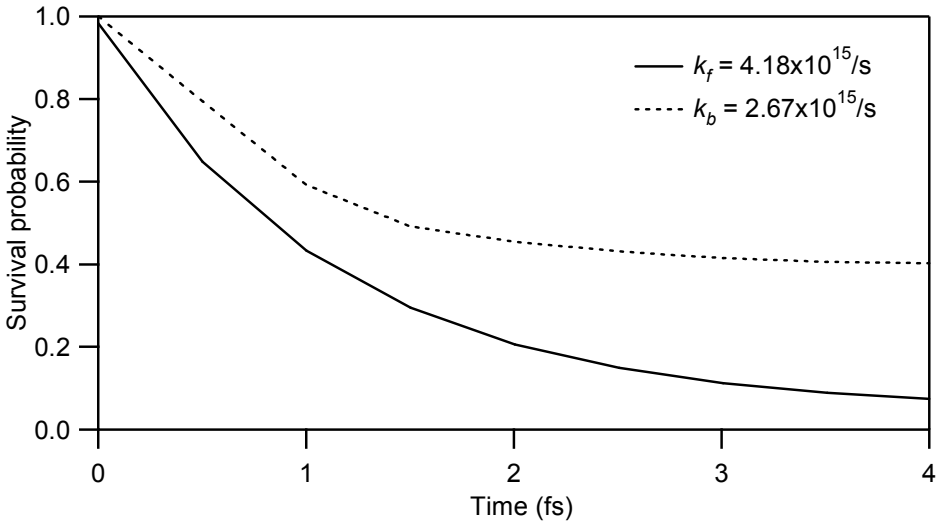

(c)

Fig. 6

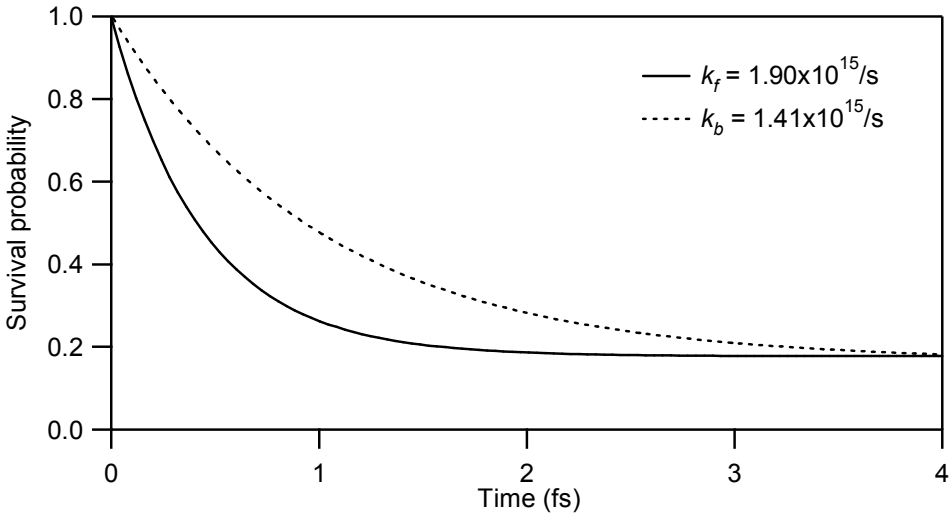

(a)

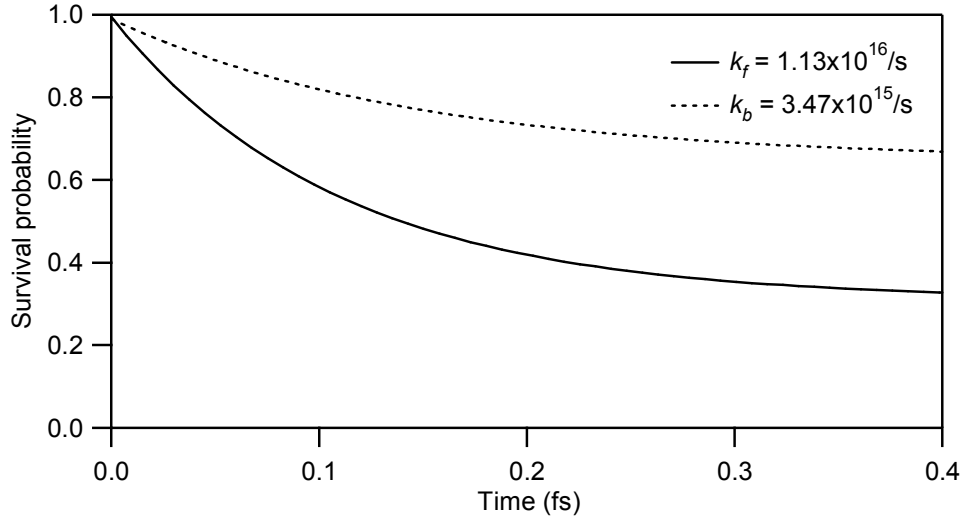

(b)

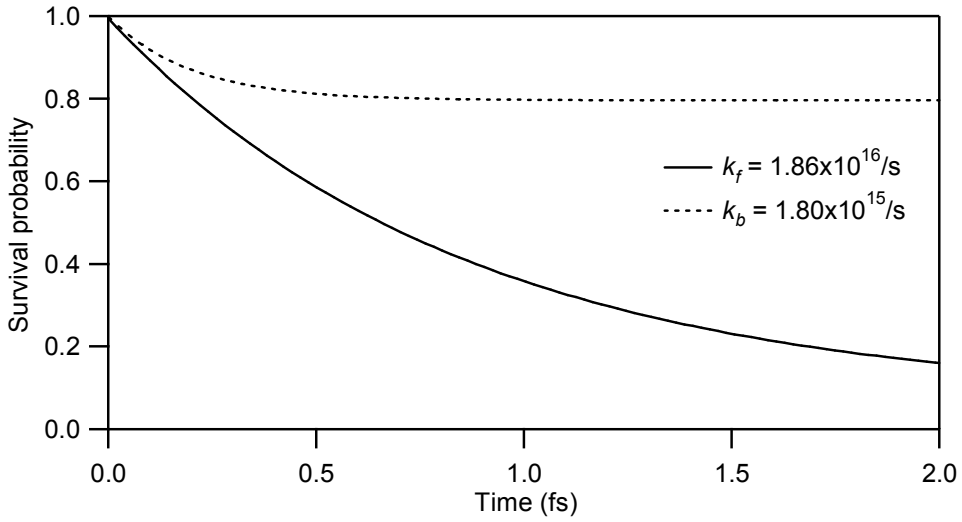

(c)

Fig. 7